Free Radical Biology and Medicine 63 (2013) 446–456

Contents lists available at SciVerse ScienceDirect

Free Radical Biology and Medicine

journal homepage: www.elsevier.com/locate/freeradbiomed

Original Contribution

A spontaneous mutation in the nicotinamide nucleotide transhydrogenase gene of C57BL/6J mice results in mitochondrial redox abnormalities

Juliana A. Ronchi [a], Tiago R. Figueira [a,**], Felipe G. Ravagnani [a], Helena C.F. Oliveira [b], Anibal E. Vercesi [a], Roger F. Castilho [a,*]

[a] Department of Clinical Pathology, Faculty of Medical Sciences, State University of Campinas, Campinas, SP 13083-887, Brazil
[b] Department of Structural and Functional Biology, Biology Institute, State University of Campinas, Campinas, Brazil

ARTICLE INFO

Article history:
Received 4 February 2013
Received in revised form
15 May 2013
Accepted 31 May 2013
Available online 7 June 2013

Keywords:
Mitochondrial NADPH
Transhydrogenation
Glutathione
Krebs cycle intermediates
Calcium
Reactive oxygen species

ABSTRACT

NADPH is the reducing agent for mitochondrial H_2O_2 detoxification systems. Nicotinamide nucleotide transhydrogenase (NNT), an integral protein located in the inner mitochondrial membrane, contributes to an elevated mitochondrial NADPH/$NADP^+$ ratio. This enzyme catalyzes the reduction of $NADP^+$ at the expense of NADH oxidation and H^+ reentry to the mitochondrial matrix. A spontaneous *Nnt* mutation in C57BL/6J (B6J-Nnt^{MUT}) mice arose nearly 3 decades ago but was only discovered in 2005. Here, we characterize the consequences of the *Nnt* mutation on the mitochondrial redox functions of B6J-Nnt^{MUT} mice. Liver mitochondria were isolated both from an *Nnt* wild-type C57BL/6 substrain (B6JUnib-Nnt^{W}) and from B6J-Nnt^{MUT} mice. The functional evaluation of respiring mitochondria revealed major redox alterations in B6J-Nnt^{MUT} mice, including an absence of transhydrogenation between NAD and NADP, higher rates of H_2O_2 release, the spontaneous oxidation of NADPH, the poor ability to metabolize organic peroxide, and a higher susceptibility to undergo Ca^{2+}-induced mitochondrial permeability transition. In addition, the mitochondria of B6J-Nnt^{MUT} mice exhibited increased oxidized/reduced glutathione ratios as compared to B6JUnib-Nnt^{W} mice. Nonetheless, the maximal activity of NADP-dependent isocitrate dehydrogenase, which is a coexisting source of mitochondrial NADPH, was similar between both groups. Altogether, our data suggest that NNT functions as a high-capacity source of mitochondrial NADPH and that its functional loss due to the *Nnt* mutation results in mitochondrial redox abnormalities, most notably a poor ability to sustain NADP and glutathione in their reduced states. In light of these alterations, the potential drawbacks of using B6J-Nnt^{MUT} mice in biomedical research should not be overlooked.

Introduction

The mitochondrial electron transport chain is a quantitatively relevant source of superoxide ($O_2^{\bullet -}$) in the majority of cell types. Physiological levels of $O_2^{\bullet -}$ and its derivatives (reactive oxygen species; ROS) are important signaling intermediates in a variety of cellular processes, while the excessive accumulation of mitochondrial ROS is implicated in the pathophysiology of many diseases [1]. To handle ROS, mitochondria possess an antioxidant system to metabolize $O_2^{\bullet -}$ into hydrogen peroxide (H_2O_2) via mitochondrial superoxide dismutase (SOD2); in turn, H_2O_2 is mainly transformed into H_2O through the action of specific peroxidases and at the expense of reduced glutathione and thioredoxin [1,2]. The ultimate reducing power for this H_2O_2-detoxifying system is NADPH, which is oxidized by specific reductases that catalyze the rereduction of the oxidized forms of glutathione and thioredoxin [2]. Therefore, the redox status of NADP is critical for the enzymatic removal of mitochondrial H_2O_2 and, in turn, for redox homeostasis [2–4].

Abbreviations: 3-OHB, 3-hydroxybutyrate; 3-OHBDH, 3-hydroxybutyrate dehydrogenase; AA, antimycin A; AcAc, acetoacetate; APAD, 3-acetylpyridine adenine dinucleotide; B6JUnib-Nnt^{W} mice, C57BL/6/JUnib mice carrying wild-type *Nnt* alleles; B6J-Nnt^{MUT} mice, C57BL/6J mice carrying mutated *Nnt* alleles; FCCP, carbonyl cyanide 4-(trifluoromethoxy)phenylhydrazone; GPx, glutathione peroxidase; GR, glutathione reductase; GSH, glutathione; GSSG, glutathione disulfide; IDH2, mitochondrial NADP-dependent isocitrate dehydrogenase; IDH3, mitochondrial NAD-dependent isocitrate dehydrogenase; Isoc, isocitrate; ME3, mitochondrial NADP-dependent malic enzyme; MPT, mitochondrial permeability transition; NAD, β-nicotinamide adenine dinucleotide; NADH, reduced form of NAD; NAD^+, oxidized form of NAD; NADP, β-nicotinamide adenine dinucleotide phosphate; NADPH, reduced form of NADP; $NADP^+$, oxidized form of NADP; NNT, nicotinamide nucleotide transhydrogenase; PCoA, palmitoyl coenzyme A; ROS, reactive oxygen species; SOD2, mitochondrial superoxide dismutase; t-BOOH, *tert*-butyl hydroperoxide; t-BOH, *tert*-butyl alcohol; TMPD, *N,N,N′,N′*-tetramethyl-*p*-phenylenediamine dihydrochloride..

* Corresponding author. Fax: +55 19 3521 9434.
** Also to be corresponded.
E-mail addresses: figueirat@yahoo.com.br (T.R. Figueira), roger@fcm.unicamp.br (R.F. Castilho).

0891-5849/$ - see front matter © 2013 Elsevier Inc. All rights reserved.
http://dx.doi.org/10.1016/j.freeradbiomed.2013.05.049

Indeed, NADPH oxidation promptly triggers mitochondrial permeability transition (MPT) in Ca^{2+}-loaded mitochondria, a process that has been implicated in mitochondrial dysfunction and cell death [5–8].

Mitochondria possess three enzymatic sources of NAPDH: NADP-dependent isocitrate dehydrogenase (IDH2), nicotinamide nucleotide transhydrogenase (NNT), and NADP-dependent malic enzyme (ME3) [3,9–11]. If pyruvate supply to mitochondria is not compromised, the last source may be negligible because ME3 displays a low affinity for malate, low maximal activity, and product inhibition by pyruvate [9]. The relative contributions of the first two sources have been proposed to be nearly 50% each [10]. Nonetheless, the functional importance of the IDH2- and NNT-mediated $NADP^+$ reduction in mammalian mitochondria under controlled conditions remains to be determined. While IDH2 catalyzes a simple dehydrogenation reaction, the NNT reaction is more complex. NNT is assembled at the inner mitochondrial membrane and couples its transhydrogenase activity to H^+ movement between the mitochondrial intermembrane space and the matrix [10,12–15], as illustrated in Fig. 1.

The electrochemical gradient across the inner mitochondrial membrane shifts the NNT equilibrium toward NADP reduction, at the expense of NAD oxidation and H^+ reentry from the intermembrane space back to the mitochondrial matrix [13,16,17]. If the electrochemical gradient is experimentally dissipated and NAD is oxidized, NNT is able to catalyze the reverse reaction [6,13,14]. In fully functional mitochondria, NNT should comprise a high-capacity source of NADPH because it may unite the capacities of several mitochondrial dehydrogenases that yield NADH. Nonetheless, the physiological roles of NNT are still gradually being revealed [3,18].

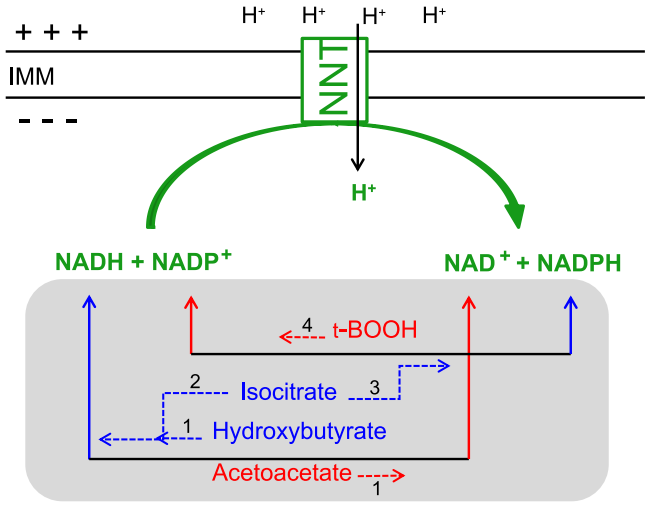

Fig. 1. Schematic of the reaction catalyzed by mitochondrial nicotinamide nucleotide transhydrogenase (NNT) and other NAD(P)-redox reactions. NNT is assembled across the inner mitochondrial membrane (IMM) and translocates H^+ to the mitochondrial matrix as $NADP^+$ is reduced at the expense of NADH on the matrix side; the electrochemical gradient across the IMM shifts the NNT equilibrium to the right. The gray box is not part of NNT reaction and is shown to depict mitochondrial NAD(P)-redox reactions (numbers **1** to **4** next to dashed arrows) that were used as a source or sink of each nucleotide involved in the NNT reaction. The reactions that had their equilibrium displaced by the addition of exogenous substrates are: (**1**) *acetoacetate+NADH+H^+ ⇌ 3-hydroxybutyrate+NAD^+*, through 3-OHBDH; (**2**) *isocitrate+NAD^+ ⇌ α-ketoglutarate+NADH+CO_2+H^+* through IDH3; (**3**) *isocitrate+$NADP^+$ ⇌ α-ketoglutarate+NADPH+CO_2+H^+*; through IDH2; (**4**) *t-BOOH+NADPH+H^+ → t-BOH+H_2O +$NADP^+$*, the overall reaction through glutathione reductase and peroxidase. In this cartoon, the blue color represents the reductants and the reduction of $NAD(P)^+$, while the red color represents the oxidants and the oxidation of NAD(P)H. NADH and NADPH, but not their respective oxidized forms, exhibit strong fluorescence signals at 366 nm excitation and 450 nm emission, which allow them to be spectrofluorometrically monitored in suspensions of isolated mitochondria.

The discovery of a spontaneous loss-of-function *Nnt* mutation in C57BL/6J mice in 2005 [19] was puzzling for at least two reasons: (i) these mice would serve as an experimental model to clarify the roles of NNT in mammalian biology; (ii) many published studies may need reevaluation, particularly those that used knockout or transgenic mice engineered on the C57BL/6J genetic background. To illustrate the latter issue, while the genetic deletion of mitochondrial SOD on C57BL/6J mice leads to death at approximately Day 15 of gestation, DBA/2 J mice (*Nnt* wild-type) exhibit an average life span of 8 days [20]. Compared to *Nnt* wild-type strains, C57BL/6J mice also present abnormal metabolic responses [21,22], including impaired glucose tolerance, which results from lowered glucose-induced insulin secretion [19,22,23]. In humans, *Nnt* mutations have been recently described as a primary cause of familial glucocorticoid deficiency. Interestingly, the C57BL/6J mice also display this phenotype [24].

Arguably, the use of C57BL/6J mice in mitochondrial studies would be especially concerning, given the likelihood of the direct impact of NNT's loss of function on the mitochondrial NADP status and the overall redox balance [3]. In light of these issues, the scientific drawbacks of using the C57BL/6J background in biomedical research have been overlooked due to insufficient comprehension about the role of NNT in mitochondrial biochemistry.

Here, we aimed to investigate the consequences of the *Nnt* mutation on the mitochondrial redox state. When compared to an *Nnt* wild-type C57BL/6 substrain (C57BL/6/JUnib), we found that isolated liver mitochondria from C57BL/6J mice displayed major redox abnormalities, including an increase in oxidized/reduced glutathione ratio, higher rates of H_2O_2 release, the spontaneous oxidation of NADPH in the absence of exogenous Krebs cycle substrates, a poor ability to metabolize organic peroxide, and a higher susceptibility to undergo Ca^{2+}-induced MPT.

Materials and methods

Reagents

The majority of the chemicals used, including malic acid, pyruvic acid sodium salt, succinic acid, rotenone, antimycin A, APAD, PCoA, acetoacetic acid lithium salt, *tert*-butyl hydroperoxide, 3-hydroxybutyric acid, isocitric acid trisodium salt, FCCP, TMPD, and NADPH, were obtained from Sigma-Aldrich (St. Louis, MO, USA). Both peroxidase from horseradish type VIA (HRP) and glutathione reductase from baker´s yeast were also obtained from Sigma-Aldrich. Malate, pyruvate, succinate, acetoacetate, 3-hydroxybutyrate, isocitrate, $NADP^+$, and NADPH stock solutions were prepared in 20 mM Hepes-KOH (pH 7.2). The fluorescent probes Calcium Green-5 N hexapotassium salt and Amplex Red were purchased from Invitrogen (Carlsbad, CA, USA).

Animals

C57BL/6J and C57BL/6/JUnib female mice were provided by the Campinas University Multidisciplinary Center for Biological Research in Laboratory Animals (CEMIB/Unicamp, Campinas, Brazil). The C57BL/6J colony was established from founders purchased from The Jackson Laboratory (Bar Harbor, ME, USA) in 2009, while the C57BL/6/JUnib colony was established in 1987 from founders supplied by the Zentralinstitut für Versuchstierzucht (ZfV) (Hannover, Germany). Based on the historic origin of these two mice colonies, C57BL/6J and C57BL/6/JUnib mice were expected to be homozygous for, respectively, mutated and wild-type *Nnt* alleles. This mutation in C57BL/6J comprises a homozygous 17,814-bp deletion in the *Nnt* gene that arose spontaneously and was named $Nnt^{C57BL/6J}$ in the MGI data bank. After genotyping as described

below, C57BL/6J and C57BL/6/JUnib were called, respectively, B6J-Nnt^{MUT} and B6JUnib-Nnt^{W} mice in this study. The use of mice and the experimental protocols were approved by the local Committee for Ethics in Animal Research (CEUA – Unicamp). Animal procedures followed the Guide for the Care and Use of Laboratory Animals published by the U.S. National Institutes of Health (NIH publication 85-23, revised 1996). The animals were kept under standard laboratory conditions (20–22 °C and 12 h/12 h light/dark cycle) with free access to a standard diet (Nuvilab CR1, Nuvital, Colombo, PR, Brazil) and tap water.

The genotypic identities between the two mice strains were evaluated by single nucleotide polymorphism (SNP) analysis. One hundred ninety-six SNPs representing 19 autosomes were selected and genotyped in the Genetic Analysis service at The Jackson Laboratory. The 196 SNPs comprise a subset of the 1638 SNPs described by Petkov et al. [25] for the identification of inbred strains. Only three differences between B6J-Nnt^{MUT} (C57BL/6J mice) and B6JUnib-Nnt^{W} (C57BL/6/JUnib mice) have been identified. C57BL/6J mice typed as follows: 09–021337884-G was T, 13–026482435-G was A, 17–058727859-G was T, while C57BL/6/JUnib typed as C, G, and C, respectively. As an example of the genotype diversity among mouse strains, 9 of the assayed SNPs revealed polymorphisms between the C57BL/6 substrains C57BL/6J and C57BL/6ByJ; in addition, 59 of the assayed SNPs revealed polymorphisms between C57BL/6J and C57BL/10 J (results not shown).

PCR assay for identification of the Nnt mutation

DNA was extracted from liver tissue by the salting-out method [26]. The B6J-Nnt^{MUT} and B6JUnib-Nnt^{W} mouse groups were genotyped using a three-primer, two-allele PCR assay to discriminate between the *Nnt* wild-type allele and the mutant allele lacking *Nnt* exons 7–11 [21]. The products of PCR amplification were 579 bp for the wild-type allele and 743 bp for the mutant allele. The products of the PCR reaction were subjected to electrophoresis in a 2% agarose gel, stained in ethidium bromide, and visualized on a UV light box using a commercial imaging system (P-Pix Image HE, Loccus Biotecnologia, Cotia, SP, Brazil).

Mitochondrial isolation

Mitochondria were isolated from the livers of female adult mice by differential centrifugation [27]. Briefly, mice livers were rapidly removed, finely minced, and homogenized in ice-cold isolation medium containing 250 mM sucrose, 1 mM EGTA, and 10 mM Hepes buffer (pH 7.2). The homogenates were centrifuged for 10 min at 800*g*. The collected supernatant was centrifuged at 7750*g* for 10 min. The resulting pellet was resuspended in buffer containing 250 mM sucrose, 0.3 mM EGTA, and 10 mM Hepes buffer (pH 7.2) and centrifuged again at 7750*g* for 10 min. The final pellets containing liver mitochondria were resuspended in an EGTA-free buffer at approximate protein concentrations of 50 mg/mL.

Heart mitochondria were also isolated for the NNT activity assay according to the following protocol. Hearts were quickly excised from the animals, washed, and minced in ice-cold isolation medium containing 210 mM mannitol, 75 mM sucrose, 1 mM EGTA, 0.1% BSA, and 10 mM Hepes buffer (pH 7.2). The heart tissue was then homogenized by hand in a glass Dounce homogenizer. The resulting homogenate was diluted with cold buffer to a final volume of 40 mL and centrifuged at 800*g* for 10 min. The supernatant was collected and centrifuged for 10 min at 6000*g* to sediment the mitochondria. The resulting pellet was suspended in 210 mM mannitol, 75 mM sucrose, and 10 mM Hepes buffer (pH 7.2) and centrifuged at 6000*g* for 10 min. The final pellet was resuspended to a final protein concentration of approximately 10 mg/mL.

The isolation procedures were performed at 4 °C or on ice. The protein concentrations of the final mitochondrial suspensions were determined by Biuret assay with bovine serum albumin as the standard.

Assay of transhydrogenase (NNT) activity

The activity of NNT was measured as previously described by Yamaguchi and Hatefi [15] and Sheeran et al. [28], with minor modifications. Briefly, the changes in differential absorbance (375–425 nm) due to the reduction of APAD, which is a NAD^+ analogue, were monitored for 5 min at 37 °C in a diode-array spectrophotometer (Shimadzu Multispec-1501, Kyoto, Japan). The assay medium contained 100 mM sodium phosphate (pH 6.5), 1 mg/mL lysolecithin, 0.5% Brij-35, 1 μM rotenone, 300 μM APAD, and 50 μg/mL heart mitochondrial protein; the reaction was initiated with 300 μM NADPH after 5 min preincubation. Heart mitochondria were chosen as the assayed sample because they yielded very low nonspecific activity backgrounds as compared to liver samples in our pilot studies. The slopes of absorbance over time were converted to nmol APAD reduced/min using the molar extinction coefficient of 5.1 $mM^{-1} \times cm^{-1}$ for reduced APAD [28]. To provide experimental controls for APAD reduction through NNT, experiments were also conducted in the presence of the NNT inhibitor PCoA (1 mM).

Assay of isocitrate dehydrogenase (IDH) activity

The enzymatic activity of NADP-dependent IDH was measured as previously described by Yan et al. [29], with minor modifications. The activity of IDH was assayed through the reduction of $NADP^+$ to NADPH in liver mitochondria (50 μg/mL) samples, with a temperature-controlled spectrofluorometer (Hitachi F-4500, Tokyo, Japan) using excitation and emission wavelengths of 366 and 450 nm, respectively, and slit widths of 5 nm. The assay medium was 33 mM Tris (pH 7.4), 0.33 mM EDTA, 1.33 mM $MgCl_2$, 0.5% Triton X-100, 0.1 mM $NADP^+$, and 1.3 mM isocitrate. The reaction was initiated by the addition of liver mitochondria.

Glutathione levels

Total glutathione (GSH) and oxidized glutathione (GSSG) levels were measured in freshly isolated liver mitochondria by the colorimetric enzymatic recycling assay described by Teare et al. [30], with minor modifications [31]. Experimental controls and standard curves were built with known amounts of GSH and GSSG.

HPLC analysis of mitochondrial NAD(P)

Oxidized and reduced forms of NAD and NADP were measured as described by Klaidman et al. [32] with the following minor modifications: an aliquot of isolated liver mitochondrial suspension (4 mg of protein) was processed; the analytical column (Luna 250 × 4.6 mm, C18 (2) 100 A, 5 μm particle size (Phenomenex, Torrance, USA)) was used in a Shimadzu HPLC (modules LC Module-1, LC-10ADVP, SIL-10ADVP, and the fluorescence detector RF-10AXL (Kyoto, Japan)). Calibration curves were built with known amounts of standards.

Incubation conditions

Measurements of mitochondrial oxygen consumption, the redox state of NAD(P), H_2O_2 production, and Ca^{2+} transport were performed at 28 °C with continuous magnetic stirring in a

standard reaction medium containing 125 mM sucrose, 65 mM KCl, 2 mM KH_2PO_4, 1 mM $MgCl_2$, 10 mM Hepes buffer, and approximately 10 μM Ca^{2+}, and pH 7.2. Other additions are indicated in the figure legends. Except for the O_2 consumption measurements, which were performed in a 1.4 mL chamber, a 2 mL final volume was used in the experiments that were performed in cuvettes.

Oxygen consumption measurements

Oxygen consumption by isolated liver mitochondria (0.5 mg/mL) suspended in standard reaction medium containing 300 μM EGTA was measured using a Clark-type electrode (YSI Co., Yellow Spring, OH, USA) in a temperature-controlled chamber equipped with a magnetic stirrer.

Mitochondrial hydrogen peroxide (H_2O_2) release

H_2O_2 release from isolated liver mitochondria was monitored by measuring the conversion of Amplex Red to highly fluorescent resorufin in the presence of added horseradish peroxidase. This assay was conducted in the presence and absence of catalase 5000 U/mL. Mitochondrial suspensions (0.5 mg/mL) were incubated in standard reaction medium containing 300 μM EGTA plus 10 μM Amplex Red and 1 U/mL horseradish peroxidase. Fluorescence was monitored over time with a temperature-controlled spectrofluorometer (Shimadzu RF-5301PC, Kyoto, Japan) using excitation and emission wavelengths of 563 and 587 nm, respectively, and slit widths of 5 nm. Data were calculated as catalase-sensitive mitochondrial H_2O_2 release.

Redox state of mitochondrial NAD(P)

Isolated liver mitochondria were suspended (1 mg/mL) in standard reaction medium supplemented with 200 μM EGTA and the changes in the redox state of NAD(P) were monitored in a spectrofluorometer (Hitachi F-4500 or Shimadzu RF-5301PC) using excitation and emission wavelengths of 366 and 450 nm, respectively, and slit widths of 5 nm. Of note, only the reduced forms of NAD(P) exhibit a strong endogenous fluorescence signal, and the discrimination between NADH and NADPH can be achieved by adding specific reductant or oxidant substrates. The addition of these substrates displaces the equilibrium of enzymatic reactions coupled to the oxidation or reduction of NAD and NADP as depicted in Fig. 1. The peroxide-metabolizing system supported by NADPH was challenged with exogenous t-BOOH, which is an organic peroxide that is metabolized through the glutathione peroxidase/reductase system [33]. As a reference, known amounts of NADPH were added to the reaction medium in the absence of mitochondria.

Measurements of mitochondrial Ca^{2+} retention capacity

The Ca^{2+} retention capacity was determined in isolated liver mitochondria (0.5 mg/mL) incubated in standard reaction medium supplemented with 0.2 μM Calcium Green-5 N as a probe. Levels of external free Ca^{2+} were measured by recording the fluorescence of this probe on a spectrofluorometer (Shimadzu RF-5301) operating at excitation and emission wavelengths of 506 and 532 nm, respectively, with slit widths of 5 nm and continuous magnetic stirring. Five minutes after the addition of mitochondria to the cuvette, boluses of 10 (pyruvate plus malate condition) or 40 nmol (succinate condition) of $CaCl_2$ were sequentially added every 2 min until the mitochondria began to release Ca^{2+} into the medium. The amount of $CaCl_2$ added prior to mitochondrial Ca^{2+} release was recorded as the mitochondrial Ca^{2+} retention capacity, thereby providing a quantitative approach to assess MPT susceptibility.

Statistical analyses

Results are shown as representative traces or as means ± standard errors (SEM) of independent experiments. Sample sizes are indicated in the figure legends. Either the Mann-Whitney (non-parametric) test or the Student *t* test was used to assess differences between two groups. $P \leq 0.05$ was defined as significant and was corrected according to Cross and Chaffin [34] when *t* test was run twice.

Results

Based on the historical origins of their colonies, the groups of B6JUnib-*Nnt*^{W} (C57BL/6/JUnib) and B6J-*Nnt*^{MUT} (C57BL/6J) mice used here were expected to be homozygous for the wild-type (full-length) and mutated *Nnt* genes, respectively [35]. With the liver as a source of genomic DNA, PCR was used to amplify a fragment of either the mutated or the wild-type *Nnt* gene. We obtained bands corresponding to products of 579 and 743 bp, respectively, for the B6JUnib-*Nnt*^{W} and B6J-*Nnt*^{MUT} mice (Fig. 2A). As previously described [21,22], this analysis confirms that B6JUnib-*Nnt*^{W} mice carry the wild-type *Nnt* alleles and B6J-*Nnt*^{MUT} mice carry mutant ones. The spectrophotometric assay for NNT enzymatic activity revealed that the mitochondria of B6J-*Nnt*^{MUT} mice display only 2% of the activity observed in B6JUnib-*Nnt*^{W} mice (Figs. 2B and 2C). In the presence of PCoA, a known competitive inhibitor of NNT [36], the NNT activity in B6JUnib-*Nnt*^{W} mice mitochondria was decreased to the levels of the B6J-*Nnt*^{MUT} mice. With respect to this NNT activity assay, it is of note that, as compared to heart, liver samples yield lower signals (absorbance slopes) (data not shown). Thus, it was our choice to use heart samples in this NNT assay performed in the beginning of this study. Nonetheless, the investigation of NNT function in fully working mitochondria (e.g. Fig. 4A) latter proved that liver mitochondria from B6J-*Nnt*^{MUT} mice do not possess NNT activity indeed.

Next, we evaluated the other significant source of mitochondrial NADPH. NADP-dependent isocitrate dehydrogenase (IDH2) activity could be upregulated as a compensatory adaptation to absent NNT activity. The evaluation of IDH2 activity indicated nearly identical activity levels between the mitochondria of B6JUnib-*Nnt*^{W} and B6J-*Nnt*^{MUT} mice (Fig. 3A). Because NADPH provides the reducing power to reduce oxidized glutathione, decreased NADPH supply in mitochondria lacking NNT activity could impair the redox status of glutathione. In fact, the measurements of reduced (GSH) and oxidized (GSSG) glutathione in freshly isolated mitochondria (which may constitute a more accurate representation of the mitochondrial redox state *in vivo*) indicated that B6J-*Nnt*^{MUT} mice possess lower ratios of reduced/oxidized glutathione (GSH/GSSG ratio) but feature similar contents of total glutathione (GSH+GSSG) as compared to B6JUnib-*Nnt*^{W} mice (Fig. 3B).

Mitochondrial respiration was evaluated before every experiment utilizing intact isolated respiring mitochondria. Neither the resting (state 4) nor the ADP-stimulated (state 3) states of mitochondrial O_2 consumption supported by either complex I- or complex II-linked substrates differed between the mitochondria of B6JUnib-*Nnt*^{W} and B6J-*Nnt*^{MUT} mice (Table S1).

In the next set of experiments, the redox status of nicotinamide nucleotides (NAD(P)) was evaluated by monitoring changes in endogenous fluorescence in response to specific oxidants and reductants added to the suspension of respiring mitochondria; the biochemical reactions implicated in these experiments are

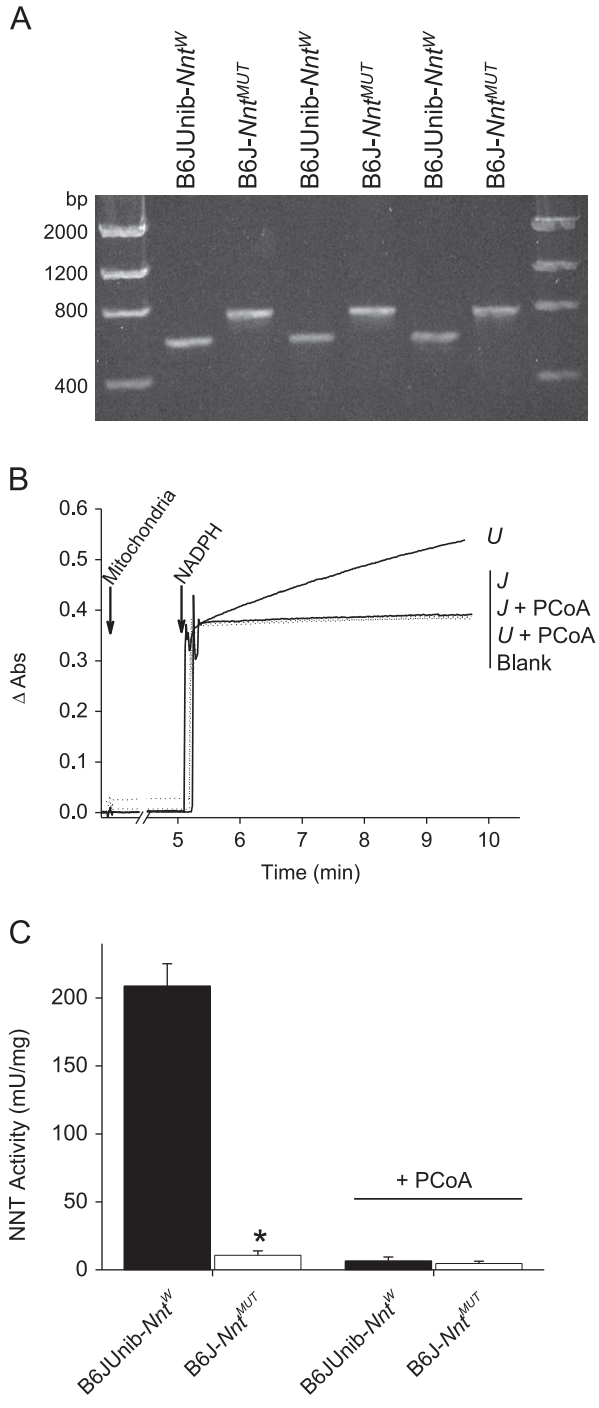

Fig. 2. *Nnt* genotyping and NNT activity. (A) DNA agarose gel analysis following PCR amplification of fragments of the mutated and wild-type *Nnt* genes from C57BL/6/JUnib (named here as B6JUnib-Nnt^{W}) and C57BL/6J (named here as B6J-Nnt^{MUT}) mice livers; the amplification products are 579 bp for the wild-type allele and 743 bp for the mutant allele. (B) Representative traces of NNT activity assayed spectrophotometrically in isolated mitochondria from B6JUnib-Nnt^{W} (*U* traces) and B6J-Nnt^{MUT} (*J* traces) mice. Following 5 min of sample preincubation (50 μg/mL), the reaction was initiated by the addition of 300 μM NADPH, while 1 mM PCoA, a known NNT inhibitor, was used as an experimental control and yielded a curve slope nearly identical to the condition lacking mitochondria (blank). (C) Means ± SEM of NNT activity in isolated mitochondria from B6JUnib-Nnt^{W} and B6J-Nnt^{MUT} mice, in the absence or presence of PCoA ($N=5$; *significantly different from B6JUnib-Nnt^{W} in the respective experimental condition at $P \leq 0.01$).

summarized in Fig. 1. The two fractions of endogenous mitochondrial fluorescence that correspond to NADH and NADPH are depicted in traces in Fig. 3C using succinate-energized

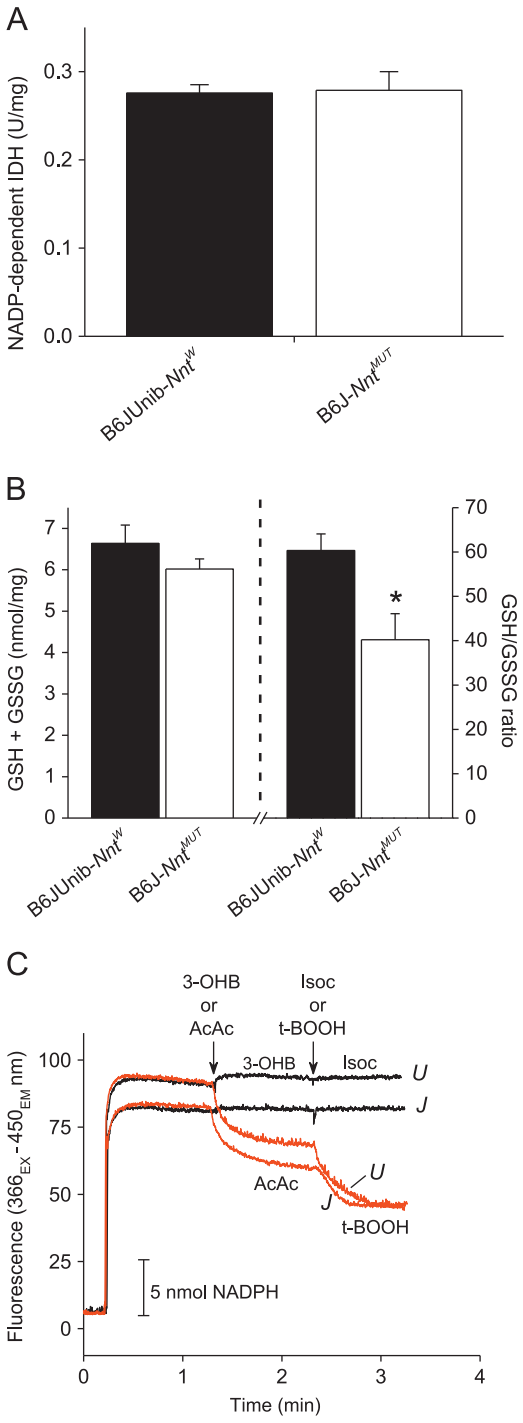

Fig. 3. Comparison of B6 JUnib-Nnt^{W} and B6J-Nnt^{MUT} mice assessing NADP-dependent isocitrate dehydrogenase (IDH) activity, GSH/GSSG ratio, and NAD(P)H fluorescence levels. (A) Activity of NADP-dependent IDH in isolated liver mitochondria; the results are expressed as means ± SEM ($N=5$). (B) Mitochondrial glutathione status. The total glutathione content (GSH+GSSG) and the reduced-to-oxidized glutathione (GSH to GSSG) ratios were determined. The results are expressed as means ± SEM ($N=9$; *significantly different from B6JUnib-Nnt^{W} at $P \leq 0.05$). C, Determination of the two fractions of the mitochondrial endogenous fluorescence that arose from NADH and NADPH, as indicated by the addition of NAD(P) reductants or oxidants ($N=4$). Traces *U* and *J* denote for B6 JUnib-Nnt^{W} and B6J-Nnt^{MUT} mice, respectively. The conditions of experiments shown in panel C are as follows: mitochondria incubated in standard medium in the presence of 1 μM rotenone and 5 mM succinate; in black traces, 5 mM 3-hydroxybutyrate (3-OHB) and 1 mM isocitrate (Isoc) were sequentially added to obtain full reduction of NAD and NADP pools, respectively; in red traces, 500 μM acetoacetate (AcAc) and 100 μM *tert*-butyl hydroperoxide (t-BOOH) were sequentially added to primarily promote the oxidation of the NADH and NADPH pools, respectively.

mitochondria in the presence of rotenone. While the fluorescence fraction corresponding to NAD was similar between the B6JUnib-*Nnt*^{W} and the B6J-*Nnt*^{MUT} mice, the fluorescence fraction linked to NADP appeared to be slightly lower in the mitochondria of B6J-*Nnt*^{MUT} mice as compared to B6JUnib-*Nnt*^{W} mice. HPLC analysis of mitochondrial stock suspensions confirmed that the total content of NADP but not of NAD was significantly lower in B6J-*Nnt*^{MUT} than in B6JUnib-*Nnt*^{W} mice (Table 1). The redox state of NADP (NADPH: NADP^{+} ratio) in mitochondrial stock suspensions was much higher in B6J-*Nnt*^{MUT} than in B6JUnib-*Nnt*^{W} mice, mainly due to a lower content of NADP^{+} in B6J-*Nnt*^{MUT} mitochondria. The latter result might be opposite to what could be expected in the absence of mitochondrial NNT activity. Nonetheless, the high concentration of mitochondrial proteins in the stock suspension leads to hypoxia/anoxia and, consequently, mitochondrial inner membrane depolarization. Under this condition, the mass action favors the reverse mode of NNT activity promoting NADP oxidation and NAD reduction in mitochondria with intact NNT function [14].

Following this general characterization of B6J-*Nnt*^{MUT} mouse mitochondria, we sought to evaluate NNT activity (transhydrogenation between NAD and NADP) in intact respiring mitochondria and the mitochondrial ability to sustain NADP in the reduced state, thereby providing the potential to metabolize peroxide. As shown in Fig. 4A, representative traces of NAD(P) fluorescence reveal reverse NNT activity in the mitochondria of B6JUnib-*Nnt*^{W} mice, a finding that was absent in the respiring mitochondria of B6J-*Nnt*^{MUT} mice. The reverse NNT reaction can be identified because of the drop in fluorescence following the depolarization by FCCP; in this situation, NADH had been already oxidized by AcAc. Thereafter, the transhydrogenation between NAD and NADP was further evaluated by the sequential addition of 3-OHB and isocitrate, which reduced NAD^{+} and NADP^{+}, respectively. In this protocol, the addition of isocitrate only increased the fluorescence in B6JUnib-*Nnt*^{W} mitochondria, thus indicating that B6J-*Nnt*^{MUT} mitochondria did not oxidize NADPH when AcAc and FCCP were present.

Remarkably, mitochondria from B6J-*Nnt*^{MUT} mice energized by succinate in the presence of rotenone exhibited a spontaneous drop in fluorescence over time (Fig. 4B); the addition of 3-OHB indicated that NADH was not oxidized in either B6JUnib-*Nnt*^{W} or B6J-*Nnt*^{MUT} mouse mitochondria, while isocitrate only elicited an increase in fluorescence (signifying the reduction of NADP^{+}) in B6J-*Nnt*^{MUT} mitochondria. However, if malate and pyruvate are the primary respiratory substrates, the mitochondria from both groups do not display spontaneous oxidation of NAD(P)H (i.e., neither 3-OHB nor isocitrate elicited an increase in fluorescence) (Fig. 4C). Such a dependence on Krebs cycle substrates (malate and pyruvate) possibly arose because isocitrate, the unique substrate

Table 1
Contents of nicotinamide nucleotides in isolated liver mitochondria from B6JUnib-*Nnt*^{W} *and* B6J-*Nnt*^{MUT} mice.

Nicotinamide Nucleotides	B6JUnib-*Nnt*^{W}	B6J-*Nnt*^{MUT}
NAD^{+}	1.69 ± 0.24	1.39 ± 0.33
NADH	0.77 ± 0.15	0.41 ± 0.09
Total NAD	2.46 ± 0.33	1.80 ± 0.37
NADH:NAD^{+} ratio	0.48 ± 0.11	0.39 ± 0.13
NADP^{+}	0.51 ± 0.07	0.18 ± 0.04**
NADPH	1.32 ± 0.15	1.12 ± 0.10
Total NADP	1.83 ± 0.19	1.30 ± 0.10*
NADPH:NADP^{+} ratio	2.81 ± 0.36	11.93 ± 3.57*

Contents of NAD(P) are expressed as nmol/mg of mitochondrial protein. Oxidized and reduced forms of NAD(P) were determined by HPLC in a single run. Data are means ± standard error (N=7–10).

** $P < 0.01$

* $P <$ 0.05 compared to B6JUnib-*Nnt*^{W}.

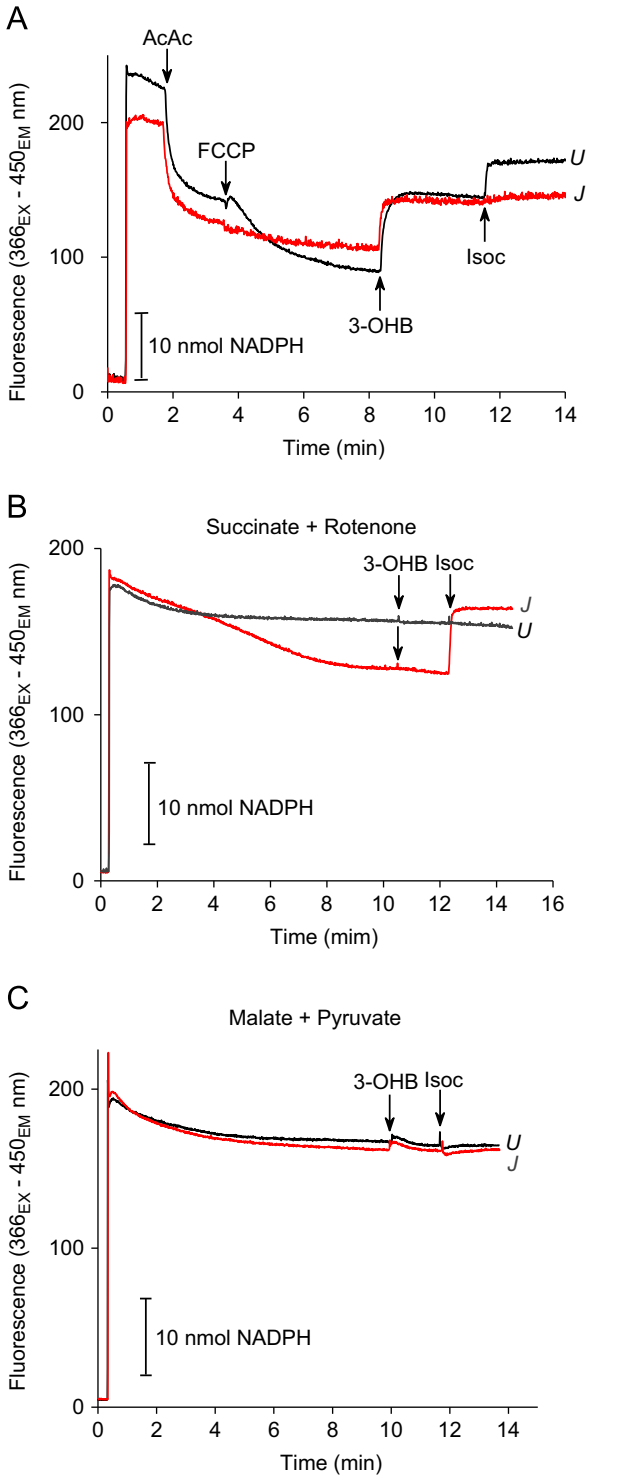

Fig. 4. Respiring mitochondria from B6J-*Nnt*^{MUT} mice do not display transhydrogenation between NAD and NADP: impact on resting NAD(P) redox state. Traces *U* and *J* denote for B6JUnib-*Nnt*^{W} and B6J-*Nnt*^{MUT} mice, respectively. (A) Mitochondria (N=5) were incubated in the presence of 1 μM rotenone and 5 mM succinate, and the following substrates were added (where indicated) to evaluate transhydrogenation between NAD and NADP: 500 μM AcAc to oxidize NADH, 1 μM FCCP to dissipate the electrochemical gradient across inner mitochondrial membrane, 1 mM 3-OHB to primarily reduce NAD^{+}, and 1 mM Isoc to selectively reduce NADP^{+} under this condition. (B) Mitochondria (N=5) from B6J-*Nnt*^{MUT} mice (*J* trace) do not sustain NADP in the reduced state when energized by 5 mM succinate in the presence of 1 μM rotenone. (C) When mitochondria (N=3) are energized by 2.5 mM malate plus 5 mM pyruvate (which feeds carbons to Krebs cycle intermediates), mitochondria from both groups of mice can sustain NAD and NADP in their fully reduced states. 3-OHB (5 mM) and 1 mM Isoc were added (where indicated) to the traces shown in panels B and C.

supporting NADP reduction in B6J-*Nnt*^{MUT} mitochondria, needs to be continuously replenished. Supplemental data indicate that malate alone does not reverse the spontaneous NADPH oxidation that occurs in B6J-*Nnt*^{MUT} mice mitochondria, even though malate could serve as an NADPH source through the actions of malic enzyme (Fig. S1).

To highlight the unique ability of NNT to unite the reducing power of endogenous Krebs cycle intermediates flowing through NAD-dependent dehydrogenases, the experiments shown in Fig. 5 were performed with mitochondria energized by TMPD/ascorbate, which is an artificial system that delivers electrons directly to complex IV of the mitochondrial respiratory chain. In Fig. 5A, three pulses of t-BOOH (an organic peroxide metabolized through the glutathione peroxidase/reductase system at the expense of NADPH) were added to mitochondria, followed by deenergization by FCCP. The addition of t-BOOH only transiently promoted NAD(P)H oxidation in B6JUnib-*Nnt*^{W} mitochondria, while B6J-*Nnt*^{MUT} mitochondria were completely unable to recover the reduced state of NAD(P) following the first single addition of t-BOOH. At the end of the traces, FCCP addition resulted in a fluorescence decay in B6JUnib-*Nnt*^{W} mice mitochondria, indicating that t-BOOH metabolism relied on NADPH regenerated through an energy-linked process (i.e., NNT). Under conditions omitting exogenous substrates for Krebs cycle dehydrogenases and the presence of FCCP from the beginning (Fig. 5B), forward NNT activity is disfavored, and mitochondria from both groups were equally unable to metabolize a single pulse of t-BOOH. However, forward NNT activity was observed (i.e., $NADP^+$ was concomitantly reduced) when NAD^+ was fully reduced by the addition of 3-OHB; this interpretation stems from the fact that isocitrate addition only promoted a minor increase in fluorescence in B6JUnib-*Nnt*^{W} mitochondria (an indication that $NADP^+$ had been indirectly reduced earlier by 3-OHB). Interestingly, the addition of 3-OHB did not increase fluorescence in B6J-*Nnt*^{MUT} mitochondria; the lack of response to 3-OHB clearly evidences the absence of NNT activity under these conditions. With regard to the fluorescence response of B6J-*Nnt*^{MUT} mitochondria to isocitrate addition in Fig. 5B, the reduction of $NADP^+$ does occur, although very slowly (Fig. S2). Conversely to Fig. 4A, in which isocitrate promptly elicits the reduction of $NADP^+$, two factors may explain the slower response observed under the conditions depicted in Fig. 5B and Fig. S2: (i) despite the mitochondrial uptake of isocitrate being impaired by deenergization, the process is stimulated by succinate and/or malate acting as a counterexchanging ion [37]; and (ii) the $NADP^+$ reduced by isocitrate is concurrently spent to metabolize the pulse of t-BOOH that was added earlier.

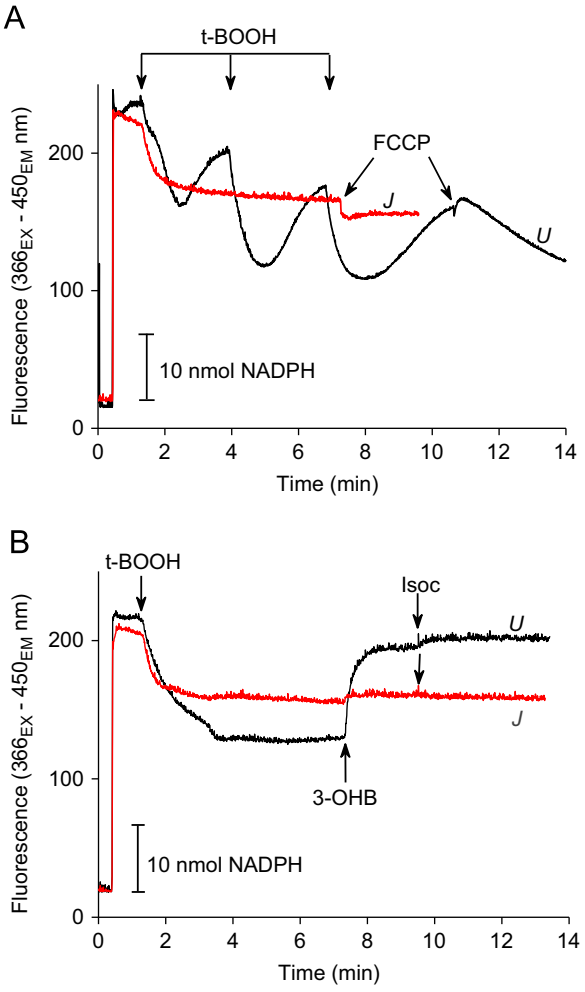

Fig. 5. The mitochondrial ability to metabolize organic peroxide in the absence of exogenous substrates is negligible in B6J-*Nnt*^{MUT} mice. Traces *U* and *J* denote for B6JUnib-*Nnt*^{W} and B6J-*Nnt*^{MUT} mice, respectively. (A) Mitochondria ($N=5$) were incubated in standard medium supplemented with 100 nM antimycin A, 1 μM rotenone, and 0.2/1 mM TMPD/ascorbate as an electron donor system to polarize mitochondria. Where indicated, pulses of 10 μM t-BOOH were added, after which 1 μM FCCP was added to collapse the mitochondrial electrochemical gradient. (B) Mitochondria ($N=4$) were incubated as in A, but 1 μM FCCP was present from the beginning; after the addition of 10 μM t-BOOH, 5 mM 3-OHB and 1 mM Isoc were added to reveal which nucleotide was oxidized during the mitochondrial detoxification of t-BOOH.

As B6J-*Nnt*^{MUT} mice are observed to thrive [35], the continuous *in vivo* supply of substrates to the Krebs cycle may be sufficient to maintain the isocitrate dehydrogenase-dependent reduction of NADPH and, thereby, H_2O_2 removal. In the presence of malate and pyruvate, B6J-*Nnt*^{MUT} mitochondria not only maintain NAD(P) in the reduced state (Fig. 4C) but are also able to metabolize exogenous t-BOOH, although at a much slower rate than in B6JUnib-*Nnt*^{W} mitochondria (Fig. 6A). The fluxes through the Krebs cycle reactions up to isocitrate formation are the likely explanation for peroxide metabolism by B6J-*Nnt*^{MUT} mice mitochondria under these conditions. Interestingly, if a high concentration of exogenous isocitrate is supplied in addition to malate and pyruvate, B6J-*Nnt*^{MUT} mice mitochondria exhibit the ability to metabolize t-BOOH at levels nearly identical to those of B6JUnib-*Nnt*^{W} mice mitochondria (Fig. 6B). The two groups differ only with respect to the higher extent of fluorescence decay promoted by t-BOOH in B6JUnib-*Nnt*^{W} mice mitochondria, which can be due to NNT-mediated oxidation of also NADH, in addition to the fact that only NADPH is oxidized in B6J-*Nnt*^{MUT} mice mitochondria. Taken together, the experiments shown in Fig. 6 indicate that mitochondria from B6J-*Nnt*^{MUT} mice possess an impaired ability to metabolize t-BOOH because they rely exclusively on NADP-dependent isocitrate dehydrogenase, whose activity is limited by the rate of isocitrate replenishment as Krebs cycle turns.

Using the Amplex Red/HRP (horseradish peroxidase) assay to measure the catalase-sensitive mitochondrial release rate of H_2O_2, we found that B6J-*Nnt*^{MUT} mice mitochondria present significantly higher rates than those of B6JUnib-*Nnt*^{W} mouse mitochondria only under the conditions of rotenone plus succinate as energy substrate. Nearly identical H_2O_2 release rates were observed between groups when energy substrates were pyruvate plus malate (Fig. 7).

Because Ca^{2+}-induced MPT is an event that is redox sensitive and may promote cell death, we determined the mitochondrial Ca^{2+} retention capacity as an assessment of mitochondrial susceptibility to MPT. Fig. 8A depicts representative experiments of mitochondria incubated in the presence of succinate plus rotenone and subjected to successive additions of Ca^{2+} pulses, to the point of MPT-mediated Ca^{2+} release. When respiring in the presence of succinate and rotenone, B6J-*Nnt*^{MUT} mice mitochondria exhibited a significantly lower Ca^{2+} retention capacity than B6JUnib-*Nnt*^{W}

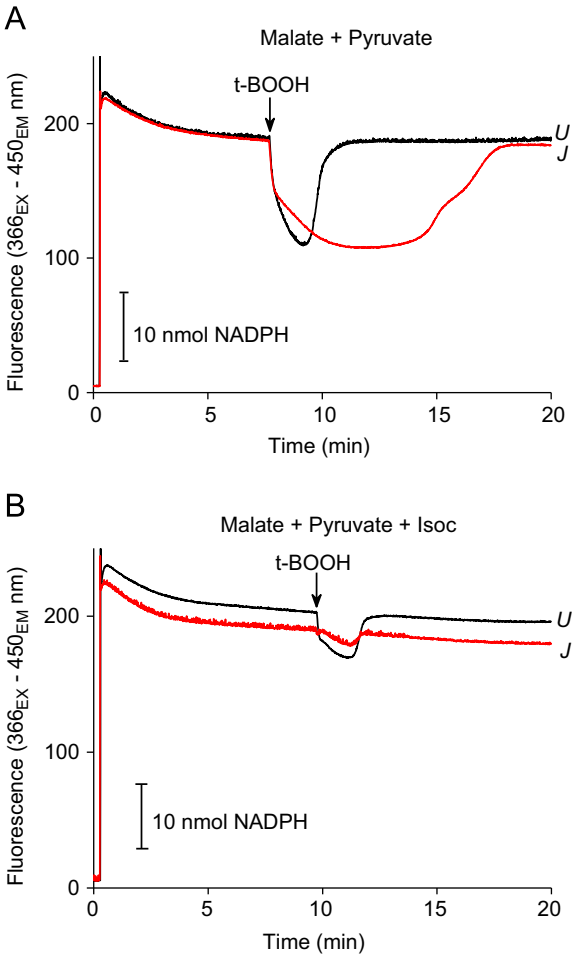

Fig. 6. Exogenous isocitrate restores the ability of B6J-*Nnt*^{MUT} mice mitochondria to metabolize organic peroxide in the presence of malate and pyruvate. Traces *U* and *J* denote for B6JUnib-*Nnt*^{W} and B6J-*Nnt*^{MUT} mice, respectively. (A) Mitochondria were incubated in standard medium supplemented with 2.5 mM malate and 5 mM pyruvate ($N=3$). (B) The same condition of A plus 1 mM isocitrate from the beginning. In both panels, 30 μM t-BOOH was added where indicated.

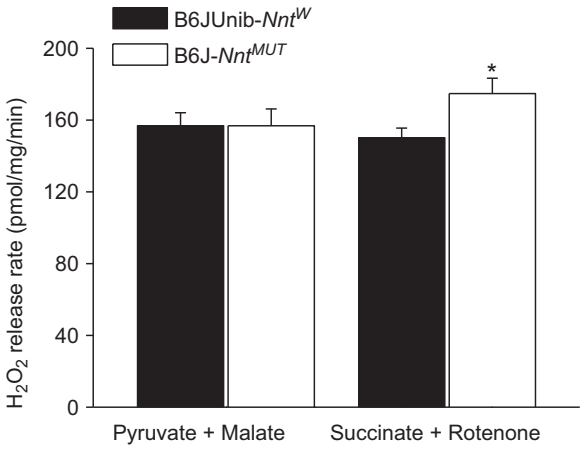

Fig. 7. Mitochondria from B6J-*Nnt*^{MUT} mice exhibit higher rates of mitochondrial H_2O_2 release. The results were calculated as catalase-sensitive H_2O_2 release rates and are expressed as means ± SEM. $N=5$; *significantly different from B6JUnib-*Nnt*^{W} in the respective experimental condition ($P\leq0.05$). B6JUnib-*Nnt*^{W} and B6J-*Nnt*^{MUT} mitochondria were incubated in standard reaction medium supplemented with either 2.5 mM malate plus 5 mM pyruvate or 5 mM succinate plus 1 μM rotenone as respiratory substrates.

mice mitochondria (Fig. 8B). However, when malate and pyruvate were used as energy substrates, there was only a nonsignificant trend for reduced Ca^{2+} retention capacity in B6J-*Nnt*^{MUT} mice mitochondria as compared to B6JUnib-*Nnt*^{W} mitochondria. It is worth noting that a higher Ca^{2+} retention capacity in mitochondria incubated with succinate and rotenone is due to rotenone's capacity to inhibit MPT [38].

Discussion

Our current findings are valuable contributions to the understanding of NNT's roles in well-coupled respiring mitochondria and to the implications of using mice with mutant *Nnt* genetic backgrounds in biomedical research. The *Nnt* mutation in B6J-*Nnt*^{MUT} mice was first described in 2005 [19] and was later shown to be associated with undetectable NNT protein expression [18] and very low NAD(P) transhydrogenase activity in detergent-permeabilized pancreatic mitochondria [23]. Using a refined NNT activity assay and a wild-type *Nnt* substrain of C57BL/6 mice as a control, we found that the specific activity of this enzyme was nearly absent in detergent-permeabilized mitochondria from B6J-*Nnt*^{MUT} mice (Fig. 2). More importantly, we demonstrated that intact respiring mitochondria from B6J-*Nnt*^{MUT} mice did not possess either forward or reverse transhydrogenation between NAD and NADP (Figs. 4A, 4B, and 5). This lack of NNT activity has several potential consequences for mitochondrial redox homeostasis that can both delineate diseases and be life-threatening under some circumstances [18–20,22,24,39]. Therefore, we designed our experiments to assess the contribution of NNT to mitochondrial detoxification of added peroxide and the main mitochondrial redox alterations due to missing NADPH provisions through NNT.

Despite IDH2 being the sole source of NADPH within B6J-*Nnt*^{MUT} mice mitochondria, its maximal activity is virtually identical between B6JUnib-*Nnt*^{W} and B6J-*Nnt*^{MUT} mitochondria (Fig. 3A). Nonetheless, using an exogenous organic peroxide (t-BOOH) that is metabolized through the glutathione-dependent system at the expense of NADPH [33], we observed that peroxide metabolism in B6J-*Nnt*^{MUT} mice mitochondria is, in fact, limited by isocitrate availability rather than IDH2 V_{max} (Fig. 6). It is worth noting that, due to several thermodynamic constraints [9], mitochondrial NADP-dependent malic enzyme was not expected to play a role in the redox status of NADP under our experimental conditions. Indeed, we did not find evidence that exogenous malate was able to reduce $NADP^+$ in B6J-*Nnt*^{MUT} mice mitochondria that exhibited spontaneous oxidation of this nucleotide (Fig. S2).

Pushed by high concentrations of exogenous malate and pyruvate feeding substrates to the Krebs cycle dehydrogenases, mitochondria from both groups sustain NAD and NADP in their fully reduced states (Fig. 4C). However, only B6J-*Nnt*^{MUT} mice mitochondria exhibited spontaneous NADPH oxidation over time (Fig. 4B) when the incubation conditions were changed to succinate as energy substrate plus rotenone (used to prevent NADH oxidation by respiratory complex I). The fully reduced state of NAD(P) in B6JUnib-*Nnt*^{W} mouse mitochondria under these conditions (Fig. 4B) may not only be the direct contribution of forward NNT activity reducing $NADP^+$ at the expense of NADH. Given that NADH turnover promoted by NNT may allow higher fluxes through Krebs cycle dehydrogenases, higher rates of isocitrate replenishment and $NADP^+$ reduction by IDH2 are expected.

Because the NADP status is highly dependent on the availability of substrates for both the NADP- and NAD-dependent dehydrogenases, the role of NNT in peroxide metabolism would be better investigated in working mitochondria lacking exogenous Krebs cycle substrates. Even succinate may support NAD^+ reduction,

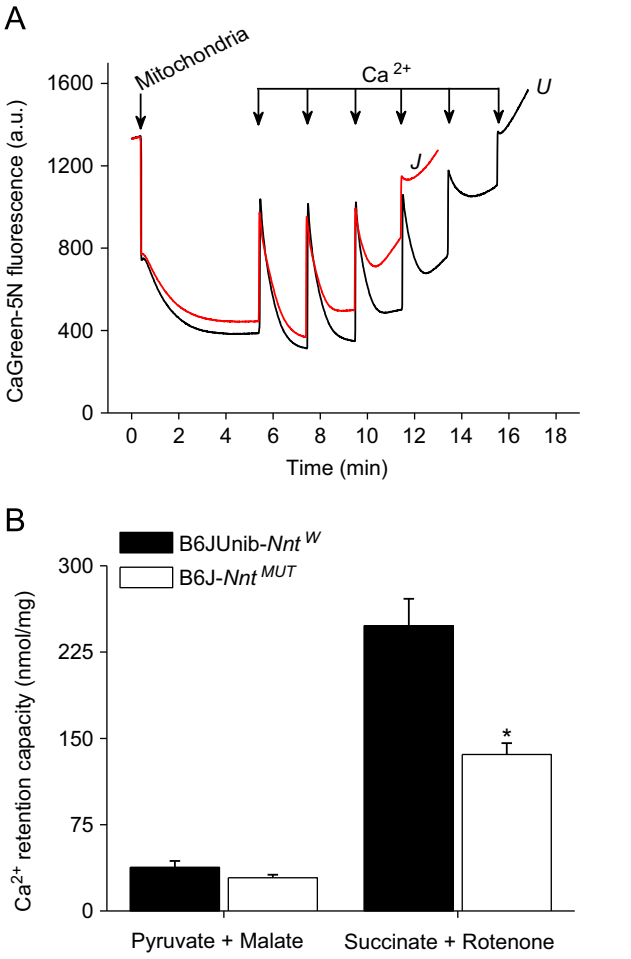

Fig. 8. Lower mitochondrial Ca^{2+} retention capacity in B6J-*Nnt*^{MUT} mice. Mitochondria were incubated in standard reaction medium supplemented with a fluorescent Ca^{2+} indicator (Calcium Green-5N) and 2.5 mM malate plus 5 mM pyruvate or 1 μM rotenone plus 5 mM succinate as respiratory substrates. To assess mitochondrial permeability transition (MPT), pulses of $CaCl_2$ (10 and 40 nmol for pyruvate/malate and succinate conditions, respectively) were added until mitochondrial Ca^{2+} release occurred due to MPT, as outlined by representative traces (succinate condition) in panel A. The sum of Ca^{2+} pulses prior to MPT opening was taken as the mitochondrial Ca^{2+} retention capacity (means ± SEM) that is shown in panel B ($N=9$ for malate+pyruvate and $N=5$ for rotenone+succinate). Traces *U* and *J* denote for B6JUnib-*Nnt*^{W} and B6J-*Nnt*^{MUT} mice, respectively. *Significantly different from B6JUnib-*Nnt*^{W} in the respective experimental condition at $P \leq 0.01$.

possibly by supplying substrate for malate dehydrogenase [33]. Hence, we used TMPD/ascorbate as an artificial system to energize mitochondria while preventing the entry of carbon skeletons into Krebs cycle intermediates (Fig. 5). Despite the insights already provided from data shown in Fig. 4B, this protocol indicated that B6J-*Nnt*^{MUT} mice mitochondria are completely unable to recover the reduced NADP state after a single addition of t-BOOH (Fig. 5A). Remarkably, the wild-type B6JUnib-*Nnt*^{W} mice mitochondria only transiently oxidized NADPH after three consecutive pulses of t-BOOH (Fig. 5A). Moreover, the ability of B6JUnib-*Nnt*^{W} mice mitochondria to detoxify t-BOOH was completely abolished when the inner mitochondrial membrane potential was collapsed by FCCP (Fig. 5B), which disfavors forward NNT activity. These findings lend clear experimental support for the notion that NNT plays a critical role in maintaining NADP in its reduced state under the conditions of low substrate availability. This enormous capacity of NNT to regenerate NADPH is likely because it unites the capacities of the Krebs cycle intermediates that support NAD^+ reduction. Conversely, in the absence of NNT (such as in the case of B6J-*Nnt*^{MUT} mice mitochondria), NADPH formation is presumed to rely solely on isocitrate availability to IDH2 reaction.

In the presence of malate and pyruvate as substrates to fuel the Krebs cycle, a condition that could support $NADP^+$ reduction by IDH2, B6J-*Nnt*^{MUT} mice mitochondria only partially restored the ability to detoxify t-BOOH as compared to B6JUnib-*Nnt*^{W} mice mitochondria (Fig. 6A). However, if the Krebs cycle reactions replenishing isocitrate are bypassed with a high concentration of exogenous isocitrate, t-BOOH metabolism is accelerated, and both groups of mice present similar responses to a t-BOOH pulse (Fig. 6B). These data indicate that the fluxes through Krebs cycle reactions may dictate the rate of isocitrate replenishment, which, in turn, limits $NADP^+$ reduction by IDH2 and, as a result, t-BOOH metabolism in B6J-*Nnt*^{MUT} mice mitochondria. Instead, B6JUnib-*Nnt*^{W} mice mitochondria have the benefit of NNT as a high-capacity NADPH source that can, at least temporarily, operate at rates exceeding the Krebs cycle flux.

Redundancies in biological systems (e.g., IDH2 as a coexisting source of mitochondrial NADPH) and the high mitochondrial capacity of metabolizing H_2O_2 (at levels in excess of their endogenous need [40]) may help us understand the viability of mice lacking NNT, although these mice exhibit disease phenotypes even under standard laboratory housing conditions [19,22,24]. Indeed, as compared to B6JUnib-*Nnt*^{W} mice mitochondria, B6J-*Nnt*^{MUT} mice mitochondria display dysfunctions related to redox imbalance (Figs. 3B, 7, and 8). Using freshly isolated mitochondria, we observed a decrease in reduced/oxidized glutathione ratio (Fig. 3B). The glutathione redox state is commonly used as an index of oxidative stress in biological systems [2]. It has been demonstrated that the suppression of NNT expression in cultured cells leads to impaired NADPH production and altered glutathione redox states [3]. We also found an increased rate of mitochondrial H_2O_2 release by B6J-*Nnt*^{MUT} mouse mitochondria (Fig. 7) only under the conditions of rotenone plus succinate as energy substrate, which could be the result of diminished H_2O_2 removal through the glutathione and other peroxidase/reductase systems due to an impaired NADPH availability (Figs. 4B and C).

The higher susceptibility of B6J-*Nnt*^{MUT} mice mitochondria to Ca^{2+}-induced MPT as compared to B6JUnib-*Nnt*^{W} mitochondria (Fig. 8) is well in line with a condition of mitochondrial redox imbalance [41]. This dysfunction was observed when mitochondria were energized by succinate in the presence of rotenone; a condition eliciting spontaneous NADPH oxidation over time only in B6J-*Nnt*^{MUT} mice mitochondria (Fig. 4B). When malate and pyruvate were used as substrates, a condition supporting reduced NADP in both groups (Fig. 4C), only a trend for a significant difference was detected between the mitochondria of B6J-*Nnt*^{MUT} and B6JUnib-*Nnt*^{W} mice (Fig. 8). Previous works by our group have pointed out that the redox imbalance and NADPH oxidation greatly stimulates Ca^{2+}-induced MPT [4–7,41–43]. MPT is of pathophysiological significance because it leads to irreversible mitochondrial dysfunction that can be followed by cell death and tissue injury [44]. Evidence for the redox regulation of MPT has been strengthened by independent studies since early reports [5,7,8,42,45]. A recent study demonstrated that cysteine 203 of mitochondrial cyclophilin D is a key redox sensor for H_2O_2-activated MPT in cells [45]. The disrupted H_2O_2 removal system and the associated increased susceptibility of B6J-*Nnt*^{MUT} mice mitochondria to MPT comprise a natural condition that lends support to the concept that redox imbalance favors MPT pore opening [41].

Importantly, the exposure of B6J-*Nnt*^{MUT} mice or NNT-deficient cells to challenging conditions reveals their higher susceptibility to degeneration or death [3,10,20,24,39], thus establishing the biological importance of NNT. A recent study has demonstrated that the loss of NNT aggravates the consequences of nonfunctinal

Bcl2l2 (an antiapoptotic mitochondrial protein), resulting in fewer live-born mice [46]. Taken together with the results from NNT-deficient cells [3], NNT loss seems to increase apoptosis susceptibility. Spontaneous abnormalities, such as glucose intolerance and glucocorticoid deficiency [19,22,24], along with the inability of B6J-*Nnt*^{MUT} mice to cope with additional stress (i.e., Bcl2l2 or SOD2 ablation, or high fat diet) [20,21,39,46], may be better understood in light of their mitochondrial redox properties reported here. In this scenario, we call attention to the innumerable studies that have used the *Nnt*-mutated C57BL/6 genetic background. Eight years after the first report on the C57BL/6J *Nnt* mutation [19], the main redox properties of mitochondria from these mice remained largely unknown. It is worth noting that this mutation spontaneously arose over 25 years ago within a mouse colony from The Jackson Laboratory [35], and this genetic background is still used worldwide. It is possible that many of the findings from these studies, especially those closely related to mitochondrial redox balance, are inaccurate due to interactions stemming from NNT deficiency and experimental manipulations.

C57BL/6J *Nnt*-mutated mice have been widely used in cardiometabolic studies, and is clear their susceptibility to experimental insults, specially diet-induced obesity and glucose intolerance [21]. *Nnt*-mutated mice on a high-fat diet exhibit higher body mass gain, adiposity, and exacerbated glucose intolerance, as compared to *Nnt* wild-type mice [21]. A mice knockout study that aimed to evaluate the role of JNK2 in acetaminophen-induced liver toxicity is a very illustrative example of scientific issues of C57BL/6J use in research, since *Nnt* mutation alone changed the acetaminophen liver toxicity [47]. Unfortunately, some studies do not properly report which C57BL/6 mice substrains were used, making data reinterpretation difficult now. The data from other studies [19–21,24,39,47–49] and the redox characterization of B6J-*Nnt*^{MUT} mice mitochondria presented here should prompt the recognition that the use of *Nnt*-mutated mice has been an undesired but neglected bias in biomedical research. With regard to genetic modifiers in C57BL/6J strain, it cannot be ruled out that other *Nnt*-linked loci on chromosome 13 may play a role in determining their known phenotype and suitability for disease models. In fact, there are major differences in phenotypes among mice strains and *Nnt*-mutated C57BL/6J mice do not always have worse outcomes than *Nnt* wild-type strains in disease models [35,39,49–51]. While, *Nnt* mutation seems to affect negatively litter survival rates [52], C57BL/6J mice exhibit a life span comparable to other strains (data available at www.jax.org) under standard laboratory housing conditions.

Current findings suggest that the B6J-*Nnt*^{MUT} mice mitochondria do not present compensatory antioxidant adaptations for NADPH supply and thus appear to be an interesting model to study the roles of NNT in physiology and disease. To achieve the aims of this study, we employed protocols from which we evaluated responses, in some cases "all-or-none phenomena," of NAD(P) oxidation and reduction within group. As stated under Materials and methods, the *Nnt* wild-type C57BL/J substrain controls (B6JUnib-*Nnt*^{W} mice) are genetically suitable, but *in vivo* interventions followed by quantitative analysis may require the generation of congenic controls. Efforts in this direction are underway in our laboratory.

We may conclude that intact respiring liver mitochondria from B6J-*Nnt*^{MUT} mice do not possess transhydrogenation activity between NAD and NADP. This lack of NNT activity results in several redox alterations, including an decrease in reduced/oxidized glutathione ratio, higher rates of H_2O_2 release, the spontaneous oxidation of NADPH in the absence of exogenous Krebs cycle substrates, poor ability to metabolize organic peroxide, and higher susceptibility to Ca^{2+}-induced MPT. Given these abnormalities and the wide use of this genetic background in biomedical research, the biological importance of the *Nnt* mutation in C57BL/6J mice and their use as experimental models should not be overlooked.

Acknowledgments

Research funding was provided by FAPESP and CNPq. T.R.F and F.G.R. are currently supported by postdoctoral and Ph.D. FAPESP fellowships, respectively. All authors disclose no conflict of interest with the content of this manuscript.

Appendix A. Supporting information

Supplementary data associated with this article can be found in the online version at http://dx.doi.org/10.1016/j.freeradbiomed.2013.05.049.

References

[1] Figueira, T. R.; Barros, M. H.; Camargo, A. A.; Castilho, R. F.; Ferreira, J. C.; Kowaltowski, A. J.; Sluse, F. E.; Souza-Pinto, N. C.; Vercesi, A. E. Mitochondria as a source of reactive oxygen and nitrogen species: from molecular mechanisms to human health. *Antioxid. Redox Signal.* **18:**2029–2074; 2013.
[2] Yin, F.; Sancheti, H.; Cadenas, E. Mitochondrial thiols in the regulation of cell death pathways. *Antioxid. Redox Signal.* **17:**1714–1727; 2012.
[3] Yin, F.; Sancheti, H.; Cadenas, E. Silencing of nicotinamide nucleotide transhydrogenase impairs cellular redox homeostasis and energy metabolism in PC12 cells. *Biochim. Biophys. Acta* **1817:**401–409; 2012.
[4] Kowaltowski, A. J.; de Souza-Pinto, N. C.; Castilho, R. F.; Vercesi, A. E. Mitochondria and reactive oxygen species. *Free Radic. Biol. Med.* **47:**333–343; 2009.
[5] Lehninger, A. L.; Vercesi, A.; Bababunmi, E. A. Regulation of Ca^{2+} release from mitochondria by the oxidation-reduction state of pyridine nucleotides. *Proc. Natl. Acad. Sci. USA* **75:**1690–1694; 1978.
[6] Vercesi, A. E. The participation of NADP, the transmembrane potential and the energy-linked NAD(P) transhydrogenase in the process of Ca^{2+} efflux from rat liver mitochondria. *Arch. Biochem. Biophys* **252:**171–178; 1987.
[7] Vercesi, A. E.; Ferraz, V. L.; Macedo, D. V.; Fiskum, G. Ca^{2+}-dependent $NAD(P)^{+}$-induced alterations of rat liver and hepatoma mitochondrial membrane permeability. *Biochem. Biophys. Res. Commun.* **154:**934–941; 1988.
[8] Costantini, P.; Chernyak, B. V.; Petronilli, V.; Bernardi, P. Modulation of the mitochondrial permeability transition pore by pyridine nucleotides and dithiol oxidation at two separate sites. *J. Biol. Chem.* **271:**6746–6751; 1996.
[9] Teller, J. K.; Fahien, L. A.; Davis, J. W. Kinetics and regulation of hepatoma mitochondrial NAD(P) malic enzyme. *J. Biol. Chem.* **267:**10423–10432; 1992.
[10] Rydstrom, J. Mitochondrial NADPH, transhydrogenase and disease. *Biochim. Biophys. Acta* **1757:**721–726; 2006.
[11] Jo, S. H.; Son, M. K.; Koh, H. J.; Lee, S. M.; Song, I. H.; Kim, Y. O.; Lee, Y. S.; Jeong, K. S.; Kim, W. B.; Park, J. W.; Song, B. J.; Huh, T. L. Control of mitochondrial redox balance and cellular defense against oxidative damage by mitochondrial $NADP^{+}$-dependent isocitrate dehydrogenase. *J. Biol. Chem.* **276:**16168–16176; 2001.
[12] Moyle, J.; Mitchell, P. The proton-translocating nicotinamide-adenine dinucleotide (phosphate) transhydrogenase of rat liver mitochondria. *Biochem. J* **132:**571–585; 1973.
[13] Rydstrom, J. Evidence for a proton-dependent regulation of mitochondrial nicotinamide-nucleotide transhydrogenase. *Eur. J. Biochem* **45:**67–76; 1974.
[14] Hoek, J. B.; Rydstrom, J. Physiological roles of nicotinamide nucleotide transhydrogenase. *Biochem. J.* **254:**1–10; 1988.
[15] Yamaguchi, M.; Hatefi, Y. Mitochondrial energy-linked nicotinamide nucleotide transhydrogenase. Membrane topography of the bovine enzyme. *J. Biol. Chem.* **266:**5728–5735; 1991.
[16] Eytan, G. D.; Carlenor, E.; Rydstrom, J. Energy-linked transhydrogenase. Effects of valinomycin and nigericin on the ATP-driven transhydrogenase reaction catalyzed by reconstituted transhydrogenase-ATPase vesicles. *J. Biol. Chem* **265:**12949–12954; 1990.
[17] Danielson, L.; Ernster, L. Energy-dependent reduction of triphosphopyridine nucleotide by reduced diphosphopyridine nucleotide, coupled to the energy-transfer system of the respiratory chain. *Biochem. Z* **338:**188–205; 1963.
[18] Freeman, H.; Shimomura, K.; Horner, E.; Cox, R. D.; Ashcroft, F. M. Nicotinamide nucleotide transhydrogenase: a key role in insulin secretion. *Cell Metab.* **3:**35–45; 2006.
[19] Toye, A. A.; Lippiat, J. D.; Proks, P.; Shimomura, K.; Bentley, L.; Hugill, A.; Mijat, V.; Goldsworthy, M.; Moir, L.; Haynes, A.; Quarterman, J.; Freeman, H. C.; Ashcroft, F. M.; Cox, R. D. A genetic and physiological study of impaired glucose homeostasis control in C57BL/6J mice. *Diabetologia* **48:**675–686; 2005.
[20] Huang, T. T.; Naeemuddin, M.; Elchuri, S.; Yamaguchi, M.; Kozy, H. M.; Carlson, E. J.; Epstein, C. J. Genetic modifiers of the phenotype of mice

deficient in mitochondrial superoxide dismutase. *Hum. Mol. Genet* **15:**1187–-1194; 2006.
[21] Nicholson, A.; Reifsnyder, P. C.; Malcolm, R. D.; Lucas, C. A.; MacGregor, G. R.; Zhang, W.; Leiter, E. H. Diet-induced obesity in two C57BL/6 substrains with intact or mutant nicotinamide nucleotide transhydrogenase (Nnt) gene. *Obesity (Silver Spring)* **18:**1902–1905; 2010.
[22] Freeman, H. C.; Hugill, A.; Dear, N. T.; Ashcroft, F. M.; Cox, R. D. Deletion of nicotinamide nucleotide transhydrogenase: a new quantitive trait locus accounting for glucose intolerance in C57BL/6J mice. *Diabetes* **55:**2153–2156; 2006.
[23] Shimomura, K.; Galvanovskis, J.; Goldsworthy, M.; Hugill, A.; Kaizak, S.; Lee, A.; Meadows, N.; Quwailid, M. M.; Rydstrom, J.; Teboul, L.; Ashcroft, F.; Cox, R. D. Insulin secretion from beta-cells is affected by deletion of nicotinamide nucleotide transhydrogenase. *Methods Enzymol.* **457:**451–480; 2009.
[24] Meimaridou, E.; Kowalczyk, J.; Guasti, L.; Hughes, C. R.; Wagner, F.; Frommolt, P.; Nurnberg, P.; Mann, N. P.; Banerjee, R.; Saka, H. N.; Chapple, J. P.; King, P. J.; Clark, A. J.; Metherell, L. A. Mutations in NNT encoding nicotinamide nucleotide transhydrogenase cause familial glucocorticoid deficiency. *Nat. Genet.* **44:**740–742; 2012.
[25] Petkov, P. M.; Ding, Y.; Cassell, M. A.; Zhang, W.; Wagner, G.; Sargent, E. E.; Asquith, S.; Crew, V.; Johnson, K. A.; Robinson, P.; Scott, V. E.; Wiles, M. V. An efficient SNP system for mouse genome scanning and elucidating strain relationships. *Genome Res.* **14:**1806–1811; 2004.
[26] Miller, S. A.; Dykes, D. D.; Polesky, H. F. A simple salting out procedure for extracting DNA from human nucleated cells. *Nucleic Acids Res.* **16:**1215; 1988.
[27] Kaplan, R. S.; Pedersen, P. L. Characterization of phosphate efflux pathways in rat liver mitochondria. *Biochem. J.* **212:**279–288; 1983.
[28] Sheeran, F. L.; Rydstrom, J.; Shakhparonov, M. I.; Pestov, N. B.; Pepe, S. Diminished NADPH transhydrogenase activity and mitochondrial redox regulation in human failing myocardium. *Biochim. Biophys. Acta* **1797:**1138–1148; 2010.
[29] Yan, H.; Parsons, D. W.; Jin, G.; McLendon, R.; Rasheed, B. A.; Yuan, W.; Kos, I.; Batinic-Haberle, I.; Jones, S.; Riggins, G. J.; Friedman, H.; Friedman, A.; Reardon, D.; Herndon, J.; Kinzler, K. W.; Velculescu, V. E.; Vogelstein, B.; Bigner, D. D. IDH1 and IDH2 mutations in gliomas. *N. Engl. J. Med.* **360:** 765–773; 2009.
[30] Teare, J. P.; Punchard, N. A.; Powell, J. J.; Lumb, P. J.; Mitchell, W. D.; Thompson, R. P. Automated spectrophotometric method for determining oxidized and reduced glutathione in liver. *Clin. Chem.* **39:**686–689; 1993.
[31] Figueira, T. R.; Castilho, R. F.; Saito, A.; Oliveira, H. C.; Vercesi, A. E. The higher susceptibility of congenital analbuminemic rats to Ca^{2+}-induced mitochondrial permeability transition is associated with the increased expression of cyclophilin D and nitrosothiol depletion. *Mol. Genet. Metab.* **104:**521–528; 2011.
[32] Klaidman, L. K.; Leung, A. C.; Adams Jr. J. D. High-performance liquid chromatography analysis of oxidized and reduced pyridine dinucleotides in specific brain regions. *Anal. Biochem.* **228:**312–317; 1995.
[33] Liu, H.; Kehrer, J. P. The reduction of glutathione disulfide produced by t-butyl hydroperoxide in respiring mitochondria. *Free Radic. Biol. Med.* **20:**433–442; 1996.
[34] Cross, E. M.; Chaffin, W. W. Use of the binomial theorem in interpreting results of multiple tests of significance. *Educ. Psychol. Measurement* **42:**25–34; 1982.
[35] Mekada, K.; Abe, K.; Murakami, A.; Nakamura, S.; Nakata, H.; Moriwaki, K.; Obata, Y.; Yoshiki, A. Genetic differences among C57BL/6 substrains. *Exp. Anim.* **58:**141–149; 2009.
[36] Rydstrom, J. Site-specific inhibitors of mitochondrial nicotinamide-nucleotide transhydrogenase. *Eur. J. Biochem.* **31:**496–504; 1972.
[37] Max, S. R.; Purvis, J. L. Energy-linked incorporation of citrate into rat liver mitochondria. *Biochem. Biophys. Res. Commun.* **21:**587–594; 1965.
[38] Li, B.; Chauvin, C.; De Paulis, D.; De Oliveira, F.; Gharib, A.; Vial, G.; Lablanche, S.; Leverve, X.; Bernardi, P.; Ovize, M.; Fontaine, E. Inhibition of complex I regulates the mitochondrial permeability transition through a phosphate-sensitive inhibitory site masked by cyclophilin D. *Biochim. Biophys. Acta* **1817:**1628–1634; 2012.
[39] Kim, A.; Chen, C. H.; Ursell, P.; Huang, T. T. Genetic modifier of mitochondrial superoxide dismutase-deficient mice delays heart failure and prolongs survival. *Mamm. Genome* **21:**534–542; 2010.
[40] Drechsel, D. A.; Patel, M. Respiration-dependent H_2O_2 removal in brain mitochondria via the thioredoxin/peroxiredoxin system. *J. Biol. Chem.* **285:**27850–27858; 2010.
[41] Kowaltowski, A. J.; Castilho, R. F.; Vercesi, A. E. Mitochondrial permeability transition and oxidative stress. *FEBS Lett.* **495:**12–15; 2001.
[42] Castilho, R. F.; Kowaltowski, A. J.; Meinicke, A. R.; Bechara, E. J.; Vercesi, A. E. Permeabilization of the inner mitochondrial membrane by Ca^{2+} ions is stimulated by t-butyl hydroperoxide and mediated by reactive oxygen species generated by mitochondria. *Free Radic. Biol. Med.* **18:**479–486; 1995.
[43] Vercesi, A. E. Stimulation of mitochondrial Ca^{2+} efflux by $NADP^{+}$ with maintenance of respiratory control. *An. Acad. Bras. Cienc.* **57:**369–375; 1985.
[44] Giorgio, V.; Soriano, M. E.; Basso, E.; Bisetto, E.; Lippe, G.; Forte, M. A.; Bernardi, P. Cyclophilin D in mitochondrial pathophysiology. *Biochim. Biophys. Acta* **1797:**1113–1118; 2010.
[45] Nguyen, T. T.; Stevens, M. V.; Kohr, M.; Steenbergen, C.; Sack, M. N.; Murphy, E. Cysteine 203 of cyclophilin D is critical for cyclophilin D activation of the mitochondrial permeability transition pore. *J. Biol. Chem.* **286:**40184–40192; 2011.
[46] Navarro, S. J.; Trinh, T.; Lucas, C. A.; Ross, A. J.; Waymire, K. G.; Macgregor, G. R. The C57BL/6J mouse strain background modifies the effect of a mutation in Bcl2l2. *G3 (Bethesda)* **2:**99–102; 2012.
[47] Bourdi, M.; Davies, J. S.; Pohl, L. R. Mispairing C57BL/6 substrains of genetically engineered mice and wild-type controls can lead to confounding results as it did in studies of JNK2 in acetaminophen and concanavalin A liver injury. *Chem. Res. Toxicol* **24:**794–796; 2011.
[48] Ripoll, V. M.; Meadows, N. A.; Bangert, M.; Lee, A. W.; Kadioglu, A.; Cox, R. D. Nicotinamide nucleotide transhydrogenase (NNT) acts as a novel modulator of macrophage inflammatory responses. *FASEB J* **26:**3550–3562; 2012.
[49] Zraika, S.; Aston-Mourney, K.; Laybutt, D. R.; Kebede, M.; Dunlop, M. E.; Proietto, J.; Andrikopoulos, S. The influence of genetic background on the induction of oxidative stress and impaired insulin secretion in mouse islets. *Diabetologia* **49:**1254–1263; 2006.
[50] Tomita, H.; Hagaman, J.; Friedman, M. H.; Maeda, N. Relationship between hemodynamics and atherosclerosis in aortic arches of apolipoprotein E-null mice on 129S6/SvEvTac and C57BL/6J genetic backgrounds. *Atherosclerosis* **220:**78–85; 2012.
[51] Barnabei, M. S.; Palpant, N. J.; Metzger, J. M. Influence of genetic background on ex vivo and in vivo cardiac function in several commonly used inbred mouse strains. *Physiol. Genomics* **42A:**103–113; 2010.
[52] Nakamura, B. N.; Fielder, T. J.; Hoang, Y. D.; Lim, J.; McConnachie, L. A.; Kavanagh, T. J.; Luderer, U. Lack of maternal glutamate cysteine ligase modifier subunit (Gclm) decreases oocyte glutathione concentrations and disrupts preimplantation development in mice. *Endocrinology* **152:**2806–2815; 2011.